Spallation reactions

J. Cugnon[1]

Spallation reactions dominate the interactions of hadrons with nuclei in the GeV range (from ~ 0.1 to ~ 10 GeV). They correspond to a sometimes important ejection of light particles leaving most of the time a residue of mass commensurate with the target mass. The main features of the experimental data are briefly reviewed. The most successful theoretical model, namely the intranuclear cascade + evaporation model is presented. Its physical content, results and possible improvements are critically discussed. Alternative approaches are shortly reviewed.

1. Introduction

There is no precise definition of the spallation. Losely speaking, this term covers the interaction of high energy hadrons or light nuclei (from a few tens of MeV to a few GeV) with nuclear targets. In a somehow restricted sense, it corresponds to the reaction mechanism by which this high energy projectile pulls out of the target some nucleons and/or light particles, leaving a residual nucleus (sometimes called spallation product). In the GeV range, this is by far the dominant interaction pattern.

Depending upon the conditions, the number of emitted light particles, and especially neutrons, may be quite large. This is, of course, the feature of outermost importance for the so-called subcritical hybrid systems [1,2]. This possibility was noticed by Lawrence in 1947 [3] after the very first experiments at the newly installed 184 inch cyclotron at Berkeley. Amusingly enough, it was also very early recognized that spallation reactions could be used for producing ^{239}Pu from depleted uranium (uranium resources were not well known at that time) and as an external source of neutrons for fission reactors [4] (already almost the concept of the energy amplifier!). The interest in spallation reactions has been recently renewed because they are of pivotal importance in the development of powerful

1. Université de Liège, Institut de Physique B5, Sart Tilman, 4000 Liège 1, Belgium.

neutron sources for various purposes:

(i) hybrid systems, be then devoted to energy production [1,2] or to incineration of nuclear wastes [5]

(ii) so-called multipurpose spallation sources devoted to irradiation studies, material structure analyses, ... [6]

(iii) future tritium production units [7].

Another interest, which has not discontinued for three decades, is related to the possibility of producing isotopes. Along these lines, let us notice the large scale investigation by astrophysicists of spallation induced nucleosynthesis and chemical evolution of the Galaxy [8]. Nuclear physicists have been interested for long by the possible production of exotic nuclei [9] and also recently by the production of exotic beams [10]. They are also interested by the possibility of producing hot nuclei [11] and studying the multifragmentation of the target [12].

Correlatively, experiments have focused on one or the other of the two main aspects of spallation reactions: energy spectrum and angular distribution of emitted light particles on the one hand and production rate of residues on the other hand. No experiment have studied the two aspects at the same time.

This review is organised as follows. In Section 2, we make a survey of the experimental data, paying particular attention to neutron cross-sections in proton-induced reactions. In Section 3, we review the most popular theoretical approach to spallation reactions, namely the intranuclear cascade (INC) + evaporation model. We briefly discuss the possible improvements of this model as well as alternative descriptions. Finally, Section 4 contains our conclusion about both experimental and theoretical knowledges and points out the need to improve them.

2. Experimental survey

2.1. Light particle emission

2.1.1. Proton induced reactions

Neutron spectra. Most of the existing measurements of neutron differential cross-sections are reported in Table 1. The quality of the measurements is not completely assessed, as the 7.5° data of references [13,14] differ by as much as a factor 2. The shape of the spectra seems rather well established. We show a typical example, namely $p + Pb$ at 800 MeV, in Figure 1. It is interesting to discuss these spectra a little bit as they provide a clue to the physics involved. There is a characteristic peak at large energy (almost the incident energy) which is quite visible at 0° and whose importance fades out with increasing scattering angle. This peak is due to quasi-elastic scattering, by which a neutron is ejected by the incoming proton and leaves the target without further interaction. This can happen in peripheral interactions only. As a matter of fact, the importance of this peak
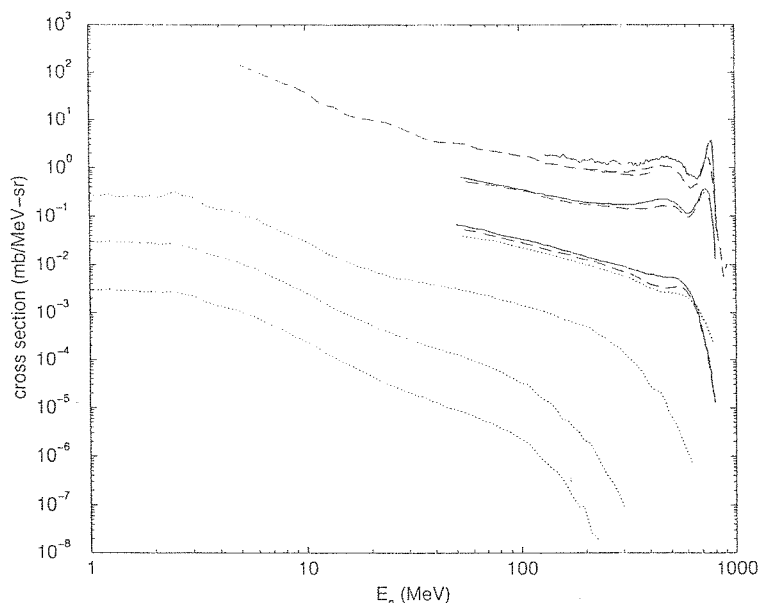
Figure 1. Representation of the available data of the neutron double differential cross-section in p (800 MeV) + Pb reactions for $0°$, $7.5°$, $30°$, $60°$, $120°$ and $150°$ from top to bottom. The cross-sections have been multiplied by a factor 10^{-n}, where $n = 1, 2, ...$ for the angle $7.5°$, $30°$, ..., respectively. The data are taken from the references indicated in Table 1.

is proportional to $A_T^{2/3}$, A_T being the target mass number. At smaller energy (down to $\sim$ 250 MeV) there is a broad bump, which also seems to disappear progressively in the "background" as the scattering angle increases. This bump is due to quasi-inelastic scattering, by which the neutron is ejected (without further interaction) by the proton which is excited to a Δ^+ resonance (see arguments below). The importance of this peak at $0°$ is proportional to $A_T^{1/3}$. The spectra display a huge peak at low energy, which is independent of the angle of emission. This is reminiscent of an evaporation process, owing to the slope parameter and the $A_T^{5/3}$ dependence.

These characteristics led Serber [15] to propose very early a two stage picture of the spallation reactions, namely a first fast stage in which the incident proton loses part of its energy by individual nucleon-nucleon scatterings and a second slow stage in which the remaining target excitation energy is released by evaporation. The component of the neutron spectra extending between the evaporation bump and the quasi-inelastic peak is presumably due to multiple collisions. We will come back to this point later on.

Proton and light charged particle spectra. Most of the existing (though not always published) proton double differential cross-sections are reported in Table 1. It is interesting to note that the shapes of these cross-sections are similar to the ones

Table 1. List of existing experimental neutron and proton data.

E_{inc} (MeV)	angle	target	references
	neutron spectra		
113	7.5°, 30°, 60°, 150°	Be, C, O, Al, Fe, W, Pb, U	NSE102(1989)310
256	7.5°, 30°, 60°, 150°	Be, C, O, Al, Fe, U	NSE110(1992)289
	7.5°, 30°, 60°, 120°, 150°	Li, Al, Zr, Pb	PRC47(1993)1647
450	30°, 45°, 60°	Be, C, Cu, Co, Bi, Pb	PRC6(1972)1496*
585	30°, 90°, 150°	C, Al, Fe, Nb, In, Ta, U	PRC36(1987)1976
597	30°, 60°, 120°, 150°	Be, B, C, N, O, Al Fe, Pb, U	NSE 115(1993)1
647	0°	Be, C, Al	PLB63(1976)35
800	0°	Al, Ti, Cu, W, Pb, U	PRC18(1978)1418
	0°	B, C, Al	PLB63(1976)35
	7.5°, 30°	Li,Al,Pb	RadEff96(1986)73
	7.5°, 30°, 60°, 120°, 150°	Li, Al, Zr, Pb	PRC47(1993)1647
	30°, 60°, 120°, 150°	Be, B, C, N, O, Al, Fe, Cd, W, Pb, U	NSE 112(1992)78
	proton spectra		
640	140°	Be, C, Al, Cu, Pb	NPA326(1979)297
800	5°−30°	C, Ca, Pb	PRC29(1984)204
	5°−30°	Li, C, Al, Ca, V, Zr, Pb	PRC21(1980)1014
	15°, 30°, 40°, 60°	C	PL100B(1981)121
	15°−150°	C, NaF, KCl, Cu, Pb	PRC24(1981)971
1000	9°−20°	C, Ca	NPA184(1972)437
2100	15°−150°	C, NaF, KCl, Cu, Pb	PRC24(1981)971

of neutron cross-sections at the same energy and for the same target. Charged pion cross-sections have been measured scarcely. Documented double differential cross-sections can be found in reference [16] at 730 MeV protons and in reference [17] for 300–580 MeV neutrons. Other measurements deal with multiplicities (see below).

There exist a few measurements of composite particle spectra, basically the low energy part. They can be found, for instance, in references [18–24]. In reference [20], it is shown that in p-nucleus collisions at 800 MeV, $d, t, \dots$ are produced by coalescence of nucleons. We will come back to the multiplicities below.

2.1.2. Other projectiles

There exists some extended measurements of the double differential cross-section for light particle emission (p, d, t, π) in neutron-induced reactions on several nuclei

(C, Cu, W, Bi) in the 300–580 MeV domain [17, 25, 26]. They show the same qualitative aspects as for incident protons.

Some studies has been made for pion-induced reactions [27]. Let us mention also the results from antiproton annihilation on nuclei [28–30], which can be considered as a multispallation process induced by the high energy pions released by annihilation. It is amusing to note that the n/p ratio is abnormally high for these reactions [29, 31]. Finally, there has been some partial measurements with light ion beams, like in references [32] (d), [33] (^{3}He), [34] (^{4}He), to cite a few examples. Reactions induced by heavier beams can still fall in the category of spallation reactions, but the mechanisms are becoming more and more complex [35].

2.1.3. Particle multiplicities

Unfortunately, very few direct measurements have been done. They can be inferred sometimes from measured total production cross-section (if the total reaction cross-section is assumed) and sometimes from the multiplicity distribution (assuming reasonable impact parameter dependence). Indicative results are shown in Table 2. A few comments are in order. The uncertainty can reach a factor 2. The indicated value of the proton multiplicities seem to be too small. The composite multiplicities are at least a factor 10 smaller than the nucleon multiplicity.

Table 2. Data on the average particle multiplicities.

type	value	average multiplicity system	references
$\langle n \rangle$	~ 10	$p(585 \text{ MeV}) + \text{Pb}$	PRC36(1987)1976
	~ 6	$p(475 \text{ MeV}) + \text{Bi}$	PLB336(1994)147
	~ 11	$p(2 \text{ GeV}) + \text{Bi}$	"
$\langle p \rangle$	1.6	$p(800 \text{ MeV}) + \text{Pb}$	PRC6(1972)1496*
	2.6	$p(2.1 \text{ GeV}) + \text{Pb}$	"
$\langle d \rangle$	~ 0.4	$p(800 \text{ MeV}) + \text{Pb}$	"
	0.75	$p(2.1 \text{ GeV}) + \text{Pb}$	"
$\langle d \rangle / \langle p \rangle$	0.1	$n(0.3-0.58 \text{ GeV}) + \text{Bi}$	NPA510(1990)774
$\langle t \rangle / \langle p \rangle$	0.01	"	"
$\langle \pi^+ \rangle$	~ 0.12	$p(730 \text{ MeV}) + \text{Pb}$	PRD 6(1972)3085
			PRC24(1981)971
$\langle \pi^- \rangle$	~ 0.06	$p(730 \text{ MeV}) + \text{Pb}$	PRD 6(1972)3085
			PRC24(1981)971

2.2. Residues

2.2.1. Introduction

Here we restrict to proton induced reactions. Most of the measurements have been done by radiochemical or activation methods. Therefore they imply the very late stages of the process, well after the cascade stage ($\sim 10^{-22}$ s), the evaporation stage ($\sim 10^{-20}-10^{-16}$ s) and even after β-decay of very short-lived emitters (this is to be contrasted to the light particle spectra, which involves the first two processes only). The experimentalists distinguish between independent yields and cumulated yields, the latter referring to isotopes that are fed by several β-decays in cascade. This is the reason why the mass spectra usually show an erratic behaviour around some general trend (see Fig. 2). Let us notice that stable isotopes are not seen by this method.
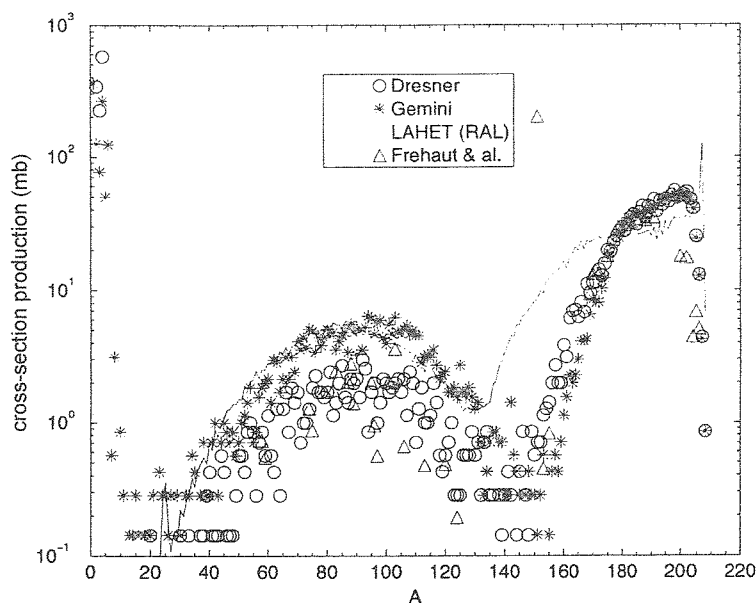

Figure 2. Residue mass spectrum for p (800 MeV) + Pb collisions. Data [40] are given by the triangles. The results of various INC + evaporation calculations are indicated by the other symbols (see text for details).

2.2.2. Survey of the experimental data

A huge amount of experimental data for light and medium-heavy targets (of astrophysical interest) has been produced by Michel's group [8]. Of particular interest for nuclear technology are the data of references [36–40] (see also Ref. [41]). One example is given in Figure 2. One uses to distinguish the various parts of the mass spectrum according to the suspected origin of the fragments. The residues

of mass close to the target one (the largest part, this part may sometimes extend very far) results from the spallation process. They are called spallation residues. The broad bump around $A \simeq 100$ corresponds to fission (fitting also into the two stage process). Light elements are produced both as fast particles ejected in the first stage and by evaporation of the remnant. The last component (the intermediate mass fragments) extends between the light fragments and the fission peak. They are produced by a simultaneous splitting of the remnant in several similar fragments or by one or several successive evaporation-like binary break-ups. This issue is not settled yet.

Semi-empirical formulae have been proposed to exhibit the general trends of the mass and isotope yields [42–44]. They generally give good results. According to reference [44], the yield for spallation products (excluding fission) can accurately be given by:

$$Y(A) = \sigma_R P(A_T) \exp(-P(A_T)(A_T - A)), \tag{1}$$

where σ_R is the total reaction cross-section, A_T is the target mass number, and where

$$P(A_T) = \exp(-0.00757 A_T - 2.584). \tag{2}$$

The isotope yields for a given isobar are given by

$$Y(Z) = n(A) \exp[-R(A)|Z_\beta(A) + \Delta - Z|^U], \tag{3}$$

where $Z_\beta(A)$ is the Z-value of the stability line, $n(A)$ is a normalization constant (to find back $Y(A)$ after integration over Z) and where

$$\Delta = 0.02703 A - 0.895. \tag{4}$$

The other parameters $R(A)$ and U (basically equal to 2) can be found in reference [44]. There are some theoretical grounds for expression (1) and the value of P [45].

3. Theoretical background

3.1. The INC + evaporation model

3.1.1. Introduction

The INC model has been suggested by Serber [15], soon after the first measurements. It is sufficient for studying nucleon and pion emission in the first stage, which dominates the energy spectra above ~ 40 MeV. The evaporation model has been developed to study compound nucleus reactions. It applies to the evolution of an excited equilibrated system and describes the emission of slow particles and the production of primary residues. A "coupling" between the two models needs be introduced to follow the fate of the system.

3.1.2. The INC model

The INC model has been used for $p, \pi, \bar{p}, ...$-nucleus and heavy ion reactions. The physical picture as well as the performances of the model has been reviewed in references [46–49]. We will limit ourselves here to a brief outline of the physical picture, of the corresponding space-time evolution of the system and of the theoretical basis.

In short, the INC model pictures the nuclear collision process as a sequence of binary baryon-baryon collisions, occurring as in free space. There are basically two lines of approach (see Fig. 3). In the first one (used in the Liège cascade [50]), all particles are propagating freely until two of them reach their minimum distance of approach d_{min}, when they may scatter if $d_{min} \leq \sqrt{\sigma_{tot}/\pi}$. In the other line of approach (like in the BERTINI code [51]), the target is seen as a continuous medium providing the particles with a mean free path $\lambda = (\rho\sigma)^{-1}$. After a path, the particle is supposed to scatter on a nucleon, which is so promoted from the continuum and which is given a mean free path as well. In the first type of approach, there is a time ordering of the collisions, but not in the second (in more modern versions, like ISABEL [52], active particles are propagated by small steps).
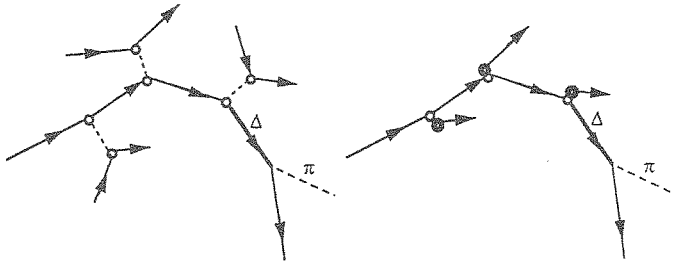

Figure 3. Schematic representation of the INC models of the first type (left) and of second type (right). In the latter case, nucleons promoted from the continuum are indicated by heavy dots.

Detailed descriptions of the INC model can be found elsewhere (see Refs. [46,53] for the first type and Refs. [51,52] for the second type). It is suffisant here to mention that features like target Fermi motion, Pauli blocking of collisions leading to already occupied states, inelastic collisions and pion production (through Δ excitation basically), (constant) mean field in the target volume are included. Collisions are described stochastically, with final states selected according to known data ($\sigma_{inel}/\sigma_{el}$ for inelasticity, $d\sigma/d\Omega$ for the scattering angle). Therefore observables are calculated by ensemble averages.

The most important space-time and physical aspects of the proton-nucleus interaction process in the GeV range, as predicted by the INC model, can be summarized as follows.

(1) The available incident energy is progressively shared by the incident particle itself, the ejectiles, the pions and the target:

$$W_p^0 = W_p(t) + K_{ej}(t) + W_\pi(t) + E^*(t), \qquad (5)$$

where $E^*(t)$ is the excitation energy of the target (similar conservation law equations can be written for momentum, baryon number and charge). As shown in reference [50], the proton travels through the target in 10 fm/c or so. It has then transferred a large fraction of its initial energy (given by $W_p^0 - W_p(t \to \infty)$) to the nucleus, which gets for a while a high excitation energy (see Fig. 4). The latter is removed to a large extent, and rather quickly (in ~ 20 fm/c), by the emission of a few fast nucleons and some pions. The remaining excitation energy is released further, much more slowly, by emission of slow neutrons, very much akin an evaporative process. Let us define E^* as the value of the excitation energy at the time where the slope changed in Figure 4.

(2) The nuclear density is depleted slightly when the proton enters the target. A kind of hole is drilled into the latter, where the density is lowered to ~ 0.75 the original value. But the target "heals" quickly, recovering a more or less uniform density much before the ejection of the fast particles is over.

(3) The relative energy transfer $((W_p^0 - W_p(\infty))/W_p^0)$ is maximum for incident energy between 1 and 2 GeV. The quantity E^* increases smoothly with energy up to 10 GeV.

(4) On the average, the proton loses energy with a rate which is universal; accordingly, we can define a nuclear stopping power, which is given in Figure 5.

(5) The number of fast ejected particles peaks around 2 GeV.

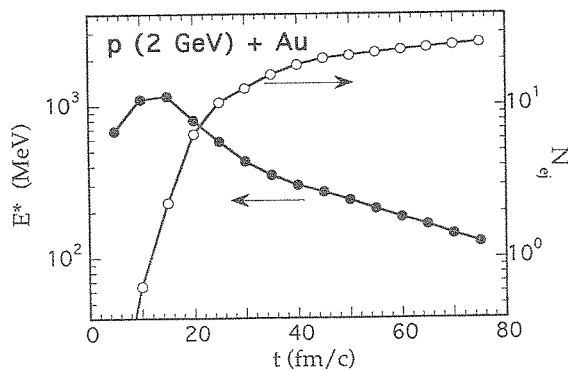(6) There are large event by event fluctuations in the observables indicated in equation (5).

Figure 4. Time evolution of the target excitation energy (left scale) and of the number of ejectiles (right scale) in $b = 2$ fm collisions for the indicated system.
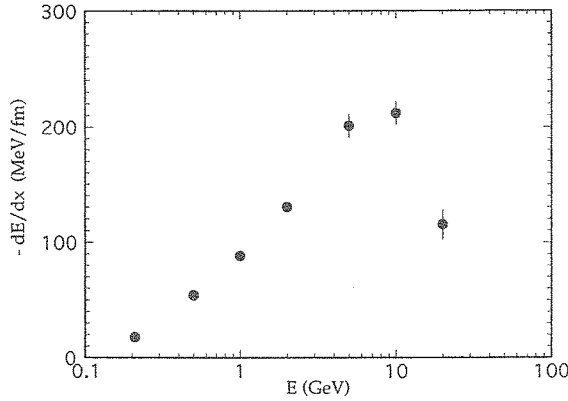
Figure 5. Nuclear stopping power for nucleons.

The necessary conditions of validity of the INC model are the following

$$\frac{\lambda_B}{v} \ll \tau_{coll} \ll \Delta t, \tag{6}$$

where λ_B is the de Broglie wavelength of the nucleons, v is the average relative NN velocity and Δt is the time interval between successive collisions. This relation expresses that the collisions involving quasi-classically moving nucleons are well separated. One has to realize that these conditions, characteristic of a dilute system, are only marginally verified in nuclear physics. They are, of course, reminiscent of the framework of the Boltzmann equation. As a matter of fact, a nuclear Boltzmann equation has recently been derived [54]. It takes the form

$$\frac{\partial f}{\partial t} + \frac{\mathbf{p}}{m} \cdot \nabla f - \nabla U \cdot \nabla_p f + \nabla_p U \cdot \nabla f =$$

$$\int \frac{d^3 p_2}{(2\pi)^3} \int \frac{d^3 p_3}{(2\pi)^3} \int \frac{d^3 p_4}{(2\pi)^3} |G(12 \to 34)|^2$$

$$\times \{f_3 f_4 (1-f)(1-f_2) - f f_2 (1-f_3)(1-f_4)\} \delta^3(\mathbf{p}) \delta(e(p)), \tag{7}$$

where f_i stands for $f(\mathbf{r}, \mathbf{p}_i, t)$, the probability of finding a nucleon with momentum $\mathbf{p}_i$ at time t and place $\mathbf{r}$. The δ-functions stand symbolically for momentum and energy conservation. In addition

$$e(p) = \frac{p^2}{2m} + U(p), \tag{8}$$

$$U(p) = \int \frac{d^3 p'}{(2\pi)^3} \langle \mathbf{p}\mathbf{p}' | G(\rho(\mathbf{r})) | \mathbf{p}\mathbf{p}' \rangle \tag{9}$$

and G is the Brueckner matrix, solution of

$$G = V + V \frac{Q}{E_{12} - H_{12}} G, \tag{10}$$

where Q is the Pauli operator acting on the intermediate states. This G-matrix describes the in-medium scattering of two nucleons. The Boltzmann equation corresponds to the limit where $U = 0$, the factors $(1 - f)$ are missing and G is replaced by the free T-matrix.

It has been shown that the INC is solving the Boltzmann equation (with the $1 - f$ blocking factors) on the average. Mathematically, the stochastic occurrence of collisions corresponds to a Monte-Carlo evaluation of the collision integral. Let us stress however that the INC is doing more than just solving the Boltzmann equation as it propagates all N-body distributions, whereas the latter deals with the one-body distribution only.

3.1.3.   The evaporation model(s)

The plural has been put purposely, as there is a large variety of models, or at least of numerical codes (for a short review, see Ref. [55]). As far as the basic ideas are concerned, all models (we restrict here to the main body of models entailing successive binary break-up) fall into one of the two following classes:

(a) the Weißkopf-Ewing model [56]. Here, the partial width for the decay $A \rightarrow B + a$, corresponding to the energy conservation equation

$$E_A^* = E_B^* + S_a + \epsilon_a, \tag{11}$$

where S_a and ϵ_a are the separation energy and the kinetic energy of particle a, is given by

$$d\Gamma = 2\pi |\langle A|T|Ba\rangle|^2 \rho(E_B^*) \frac{V k_a^2 dk_a}{(2\pi)^3} . \tag{12}$$

It can also be written as

$$d\Gamma = \sigma(aB \rightarrow A) \frac{2m_a}{(2\pi)^3 \hbar^2} \frac{\rho(E_B^*)}{\rho(E_A^*)} \epsilon_a d\epsilon_a, \tag{13}$$

by using

$$\sigma(aB \rightarrow A) = \frac{2\pi}{\hbar} \frac{|\langle A|T|Ba\rangle|^2 \rho(E_A^*)}{\hbar k/m_a V} . \tag{14}$$

In these equations ρ is the density of states and $\sigma(aB \rightarrow A)$ is the inverse capture cross-section. For the sake of clarity, we have disregarded the spin of the particles and the possible excitation of particle a;

(b) the transition state method (TSM). In this case, it is assumed that the transition probability is entirely given by the properties of the barrier appearing in the variation of interaction energy between B and a with the coordinate representing their separation. More precisely, the transition rate is assumed to be given by the ratio of the number of states of the system $(B + a)$

at the barrier occupied per unit time in an energy interval and the number of initial states in the corresponding energy interval:

$$\omega = \frac{d\Gamma}{\hbar} = \frac{\rho(\tilde{E}_B^*)d\tilde{E}_B^*(dp_a dq_a/2\pi\hbar)/dt}{\rho(E_A^*)dE_A^*} . \tag{15}$$

Note that this time, $\tilde{E}_B^*$ and ϵ_a (equal to $p_a^2/2m$) are the energy of the so-called activated complex, namely the system $B + a$ at the barrier, and the kinetic energy of particle a along the coordinate q_a *at the barrier*, respectively. One has $E_A^* = \tilde{B} + \tilde{E}_B^* + \epsilon_a$, where $\tilde{B}$ is the height of the barrier. Because of the latter relation and $dq_a/dt = v_a = p_a/m_a$, one obtains

$$d\Gamma = \frac{1}{2\pi}\frac{\rho(\tilde{E}_B^*)}{\rho(E_A^*)}d\epsilon_a. \tag{16}$$

This method was originally proposed by Bohr and Wheeler [57] for the case of fission.

In both methods, a close expression for the total emission width (in channel $B + a$) can be obtained if a simplified expression is assumed for the density of states, namely

$$\rho \propto e^{2\sqrt{aE^*}}, \qquad E^* = aT^2. \tag{17}$$

One then obtains

$$\Gamma = \frac{2m_a\sigma(aB \rightarrow A)}{(2\pi)^3\hbar^2}T^2 e^{-\frac{S_a}{T}} \tag{18}$$

and

$$\Gamma = \frac{T}{2\pi}e^{-\frac{\tilde{B}}{T}}, \tag{19}$$

for method (a) and method (b), respectively.

   Model (b) was extended to any binary decay by Moretto [58, 59] and by Swiatecki [60], who first advocates its use for light particle emission. The two methods are differing on three points:

(i) in equation (12), the quantity $\sigma 2m_a\epsilon_a/2\pi h^2 = \sigma/(2\pi/k^2)$ is nothing but a transmission factor. The latter is missing in equation (15). Swiatecki proposed to introduce a similar factor for the transmission of the one-dimensional barrier;

(ii) the 3D phase space is used in (a), whereas only one degree of freedom is considered in (b);

(iii) the density of states of the activated complex is used in (b), whereas the (free) density of states of B is introduced in (a).

There is a spectacular difference between the numerical values of the widths (or lifetimes) predicted by the two models, as illustrated in reference [61]. It is not easy to trace back the origin of these differences. Furthermore, especially for model (a), the lifetimes are abnormally small at large excitation energy (note that for calculating the evaporation yields, only relative values are needed). Obviously, what is missing in the derivation of both models (a) and (b) is the time description of the system. Indeed, it is implicitly assumed that the system does not change significantly on the time scale t_{ev} for evaporating a particle. Furthermore, it is assumed that the initial state can be described by a stationary state. These assumptions require

$$t_{ev} \ll t_{eq}, t_{sp},\qquad(20)$$

where t_{eq} is the equilibration time, *i.e.* the time necessary for a fluctuation to be damped and $t_{sp} \simeq R/v_F$ is the time necessary for a nucleon to cross the system. This is a very stringent condition at high excitation energy. An additional condition is that the system is not too much perturbed by the evaporation process itself. This does not seem to be the case when neutron emission competes with slow fission [55].

Another missing ingredient is the probability for preformation of the emitted particle. This is probably more and more important as the mass of the emitted particle is increasing. This is probably one of the reasons for the difference between the results for the mass yields in the two models. In general, models (a) give satisfactory results for light particles but underestimates the yield for intermediate mass fragments. The converse is true for models (b) in general.

Apart from these open problems, the evaporation models are crucially sensitive to the parameterization of the density of states. At very low excitation energy, this quantity has been determined systematically by counting narrow resonances [62]. Otherwise, one has to rely on calculations. Only very limited microscopic calculations have been done. Most of other theoretical investigations are based on the single-particle model. Except at very low energy, all predict the following form:

$$\rho = Ca^\alpha \frac{e^{2\sqrt{aE^*}}}{E^{*\beta}},\qquad(21)$$

but disagree on the exponents α and β. Pure single-particle models predict $E^* = aT^2$ and $a = A/16$. The systematics at low energy [62] shows important shell effects and strong structure effects: it indicates $a \simeq A/8$ when shell effects are averaged out. Using single-particle models with a realistic potential gives a more reasonable value of a [63] and predicts a decrease with increasing value of T. However, one has to stress that this parameter enters through the exponential and only a small modification of it may induce a strong effect on the results.

3.1.4. Practical applications. Possible improvements

An extensive comparison between the predictions of the INC + evaporation model and the experimental data described in Section 2 is beyond the scope of this review. We will only give an idea of the kind of agreement that can be achieved, indicate how INC effects can be disentangled from evaporation effects and look for possible improvements.

Figure 6 shows the predictions of a calculation [64] based on the Bertini cascade and a standard evaporation code [65], compared to the standard data of reference [66]. The agreement is globally satisfactory. Results with the Liège cascade are equally good [67], as shown in Figure 7 on another example. It is interesting to note (see Fig. 8) that the neutron spectrum can be split almost abruptly in a low energy component due to the evaporation and a high energy component due to the INC stage. A close examination of Figure 8 reveals that taking the INC contribution alone for neutron energy larger than 15 MeV and the evaporation contribution alone for less than 15 MeV would give an agreement of as good quality (if not better in this particular case) as the one obtained with the full calculation. The agreement seems to be equally good for the INC component and the evaporation component as well, deviations being not larger than a factor 2. However, the integrated INC contribution is sizably smaller than the evaporation contribution. To fix the ideas, the ratio between the two contributions is ~ 0.1 at 150° and ~ 0.55 at 30°. In absolute value the agreement on the evaporation
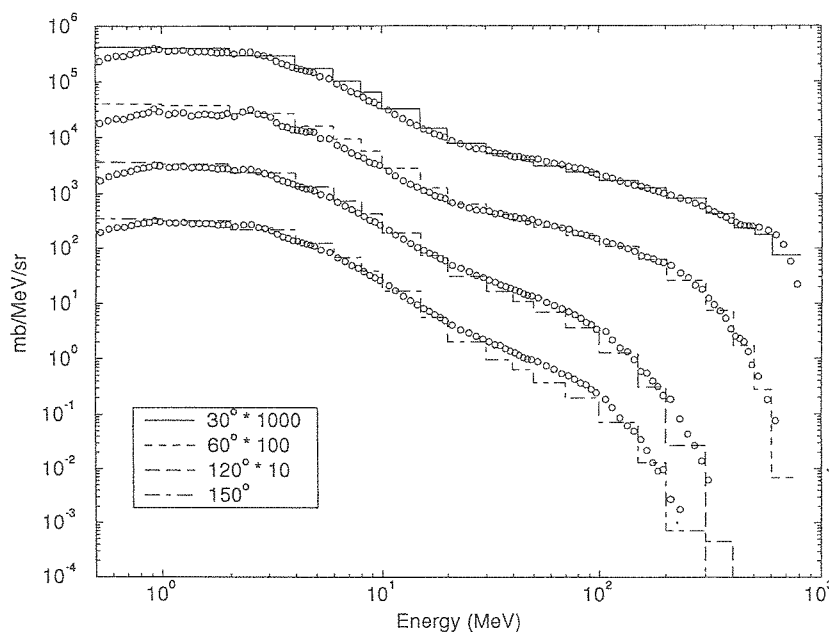
Figure 6. Neutron double differential cross-section data (Ref. [66]) compared with the INC calculations of reference [64].
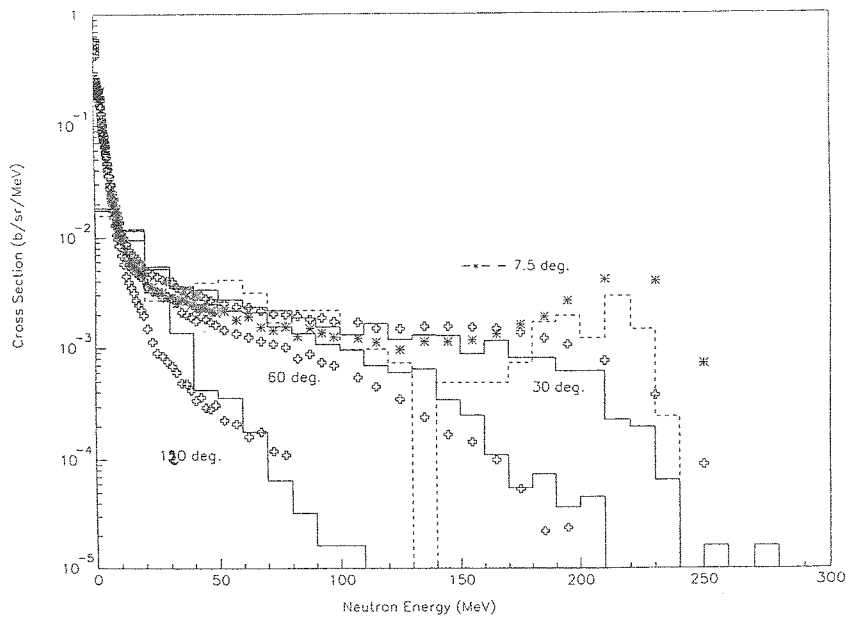
Figure 7. Comparison of neutron double differential cross-section data (Ref. [14]) with the predictions of the Liège INC model (from Ref. [84]). Only the cascade component is shown.
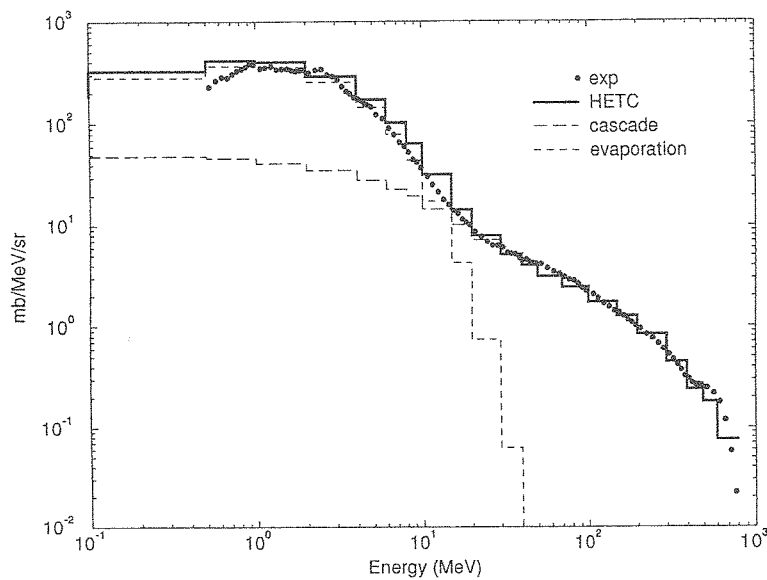

Figure 8. Splitting of the neutron spectrum in cascade and evaporation contributions (from Ref. [64], by courtesy of O. Bersillon).

is much more important than the agreement on the INC component. Concerning the neutronics of the hybrid systems, deviations of a factor 2 are not acceptable. Therefore these calculations have to be improved (note that the compatibility of the data have also to be improved!). In view of these considerations, it would be more appropriate and more efficient to improve the evaporation model than the cascade model. It is however fair to recall that high energy neutrons are producing secondary reactions in a thick target and thence an error on their yield is expected to be amplified in transport calculation in macroscopic matter. The importance of the evaporation contribution is also impressively underlined by reference [11]: the average total neutron multiplicity is about 4 times the multiplicity of the neutrons coming from the INC stage.

The importance of the evaporation is even more crucial for the description of the residue mass spectrum. In Figure 1, the results of two calculations [67], both using the Liège cascade, but different evaporation codes, are shown. Globally, they both give reasonable agreement (in the standards of heavy ion physics, for instance). However, the discrepancy between the two calculations is much larger than the accuracy with which the yield of some radioactive isotopes need to be known for radiotoxicity evaluations [6].

Of course, the separation between INC and evaporation is somewhat articifial and model dependent. This bring us to the discussion of the "coupling" between the INC code and the evaporation one. Usually, a criterion is chosen to stop the cascade process at some stage. The residue mass, charge, excitation energy and sometimes angular momentum are evaluated and used as input for the subsequent evaporation calculation. This should be done event by event in principle. The necessity to flip to evaporation model is not just a matter of convenience (running the cascade for a long time would be time-consuming) but is dictated by the fact that the evaporation process involves structure effects (shell effects and configuration mixing, as we mentioned above) that are not taken into account by the cascade, which embodies average single-particle properties only. For the Liège cascade, the arbitrariness in the choice of the stopping criterion has tentatively been minimized, as it is based on physical arguments. In the careful analysis of reference [68], it is noticed that the time evolution of the excitation energy is changing slope at some well defined time t_{sl} ($\sim$ 30 fm/c in the case of Fig. 4) and that this change is correlated in the time variation of other quantities like the number of ejectiles, the number of participants and the mean energy of the ejectiles. At this time, the target density is more or less uniform again and the emission of nucleons is fairly isotropic. The further evolution of the system within the cascade is akin to evaporation (see Fig. 4). However the time scale is too short, compared to the one predicted by the Weißkopf-Ewing model for instance. The quantity t_{sl} thus looks as the appropriate stopping time. It cannot be defined more accurately than, say, 5 fm/c. It has been checked that the particle spectra are not sensitive to such a variation. Stopping a little bit earlier (later) generates a little bit less (more) neutrons of energy around 20 MeV in the cascade, but leaves a little more (less) excited residue, which evaporates a little bit more (less) neutrons in the same energy range. As for the residues, the effect is presumably more important.

The stopping criteria in the Bertini model (also in ISABEL) pertains to the largest kinetic energy of the nucleons remaining in the target. The process is stopped when this quantity is smaller than a certain value, chosen freely (40 MeV is often quoted). It is not clear whether this criterion can be translated in a time criterion in the Liège cascade. It seems that this would correspond to a value of t_{sl} much smaller than the one recommended in reference [68], too short for the remnant be considered as equilibrated. This might be the origin of the peak predicted by the LAHET calculation (see Fig. 2). In this cascade calculation, the remnant is left most of the time with a huge excitation energy, leading to a strong depletion of the mass spectrum below this peak.

Let us discuss briefly the possible improvements of the INC+evaporation model. For the INC itself, one may distinguish the intrinsic possible improvements, remaining in the basic semi-classical framework of the models and those that are supposed to enlarge this framework. Most of the first ones can be guessed from the nuclear Boltzmann equation (3.3). They involve using in-medium cross-sections [69–71] for both elastic and inelastic scattering, using energy (and density) dependent mean field and the corresponding phase space distortion in the final states of binary collisions [71]. Additional improvements pertain to in-medium properties of the resonances and to the treatment of the Pauli principle, which works on the average only. The improvements of the second type mentioned above have not been investigated yet, but they can be identified as coming from the properties of strongly interacting fermions. Some of them have been studied in detail for nuclear matter at equilibrium and even to some extent for ground state nuclei [72,73]. Nucleons are no longer on the energy shell: there is no definite relation between the energy and momentum. For a given value of the latter, there is a distribution of the values of the former, and conversely. For our purpose, this has at least two consequences. The momentum distribution of the target nucleons has a tail above the Fermi momentum (even though the energy does no extend above the Fermi energy). Collisions between off energy-shell nucleons induce memory effects in the collision process [74,75]. Related effects may influence the quasi-elastic and quasi-inelastic processes.

3.2. Alternative approaches

In heavy ion physics, the INC model has given way to other approaches like QMD [76] or AMD [77], which present improvements of the mean field treatment, as especially for the first one, and of the Pauli principle as for the second one. In spallation reactions, where the motion in phase space is much more modest, these improvements are not so crucial. Furthermore, the calculations in these new approaches are very time-consuming and it is not realistic to insert them in large transport codes. Of more direct interest are the exciton (or pre-equilibrium) model and the FKK model. We will discuss the latter shortly.

The exciton model was initiated by Griffin [78] and Blann [79] and exists now with many degrees of sophistication (see Ref. [80]). The essential feature is the description of the time dependent excitation energy of the nucleus by an evolving

population of the particle-hole pairs. A single-particle density has to be postulated, as well as an initial population. The population of the n exciton state follows a set of master equations of the type

$$\frac{dP_n(t)}{dt} = P(n-2,t)\lambda_+^{n-2}(E) + P(n+2,t)\lambda_-^{n+2}(E)$$
$$- P(n,t)\left[\lambda_+^n(E) + \lambda_-^n(E)\right] - P(n,t)\lambda_{ev}^n(\epsilon), \tag{22}$$

where $\lambda_+^p(\lambda_-^p)$ is the transition from state p to state $p+2(p-2)$, and where λ_{ev}^n is the probability to evaporate a particle of energy ϵ from state n. Only $p \to p \pm 2$ transitions are allowed in reminiscence of the two-body character of nucleon-nucleon interaction. This model has been applied only below 100 MeV where the initial configuration may be chosen rather simply. According to a suitable choice for the end of the process, a good agreement with the experiment may be achieved. The latter is often obtained with an adjustable choice of the transition probabilities. Let us notice that more sophisticated master equations may be used, based on a realistic single-particle spectrum and single-particle state occupation numbers. Recently, the exciton model has been used as an intermediate step between the INC and the evaporation model [81]. This procedure introduces several extra parameters, as the times for passing from one stage to the other and the transition probabilities. The only advantages are the use of a discrete single-particle spectrum (instead of a continuous one in the INC) and the possibility to include a simple (but non parameter free) way for the emission of composites.

The multistep compound and multistep direct theory of Feshbach, Kerman and Koonin [82], also assumes that the collision proceeds by stages of increasing complexity, but tries to preserve some quantum mechanics features. The projectile enters the nucleus and produces a $2p - 1h$ state. By further interactions it can produce $(n+1)p - nh$ configurations, increasing (or decreasing) the value of n by one unit at each step. A distinction is made between multistep compound process where all particles are bound and multistep direct where at least one particle is in the continuum. For multistep compound processes, the transition probabilities are assumed to have random phases whereas a constructive interference is assumed for transition keeping the same direction for the nucleons. Complicated expressions can be written for the cross-sections (see Ref. [80]). In practice only two or three steps can be handled microscopically in as much as the transition probabilities should be calculated by the DWBA method. Very promising results [83] are obtained below 50 MeV or sometimes 100 MeV, an energy range where this method is expected to be restricted for practical reasons.

4. Conclusion

We have seen that the bulk of the experimental data concerning spallation reactions can be understood in the frame of the INC + evaporation model, which embodies the division into a first rapid cascade stage (dominated by nucleon-nucleon

collisions) and a slow evaporation stage. However finer details, necessary for building a reliable highly predictive transport code for propagation inside matter, are still to be worked out, both experimentally and theoretically. Discrepancies between overlapping data may be as large as a factor 2 and have to be removed. On the theoretical side, the INC model has to be improved, particularly concerning the quasi elastic and quasi inelastic components. But a more important effort has to be put on the improvement of the evaporation codes, both on the formulation of the model and on the ingredients. Finally, one should not forget that good models for composite production are still lacking.

Note added in proof: Since the completion of the work, the discrepancy between neutron spectra in Figure 1 has been resolved by the recent measurements of Saturne [85], which are well reproduced by the INC Liège model. The measurements of the residue production cross-sections are being considerably improved by the current experiments at GSI using the inverse kinematics techniques. For a preliminary account, see reference [86].

Références

[1] C.D. Bowman et al., NIM A **320**, 336 (1992).

[2] C. Rubbia et al., Conceptual design of a fast neutron operated high power energy amplifier, preprint CERN/AT/95-44(ET), 1995.

[3] C.M. van Atta, A brief history of the MTA project (unpublished)

[4] W.B. Lewis, Atomic energy of Canada report DR-24, 1952.

[5] M. Spiro et al., The INCA project, Journees GEDEON, Jouy-en-Josas, France, May 1996.

[6] F. Atchison, Proc. Meeting on Targets for Neutron Beam Spallation Sources, KFA-Jülich, Jül-Conf. 1980, p. 17.

[7] J.L. Flament, Proc. 2nd International Workshop on Spallation Material Technology, edited by F. Carsughi et al., KFA-Jülich, Jülich, 1997, p. 71.

[8] R. Michel et al., NIM B **103**, 183 (1995).

[9] P.G. Hansen, Ann. Rev. Nucl. Part. Sci. **29**, 69 (1979).

[10] B. Jonson, D.D. Warner, in *Physics and Tecniques of Secondary Nuclear Beams*, edited by J.F. Bruandet, B. Fernandez, M. Bex (Éditions Frontières, Gif-sur-Yvette, 1992).

[11] L. Pienkowski *et al.*, Phys. Lett. B **336**, 147 (1994).

[12] N.T. Porile *et al.*, Phys. Rev. C **39**, 1914 (1989).

[13] S. Stamer *et al.*, Phys. Rev. C **47**, 1647 (1993).

[14] M.M. Meier *et al.*, Radiat. Eff. **96**, 73 (1986).

[15] R. Serber, Phys. Rev. **72**, 1114 (1947).

[16] D.R.F. Cochran *et al.*, Phys. Rev. D **6**, 3085 (1972).

[17] R. Büchle *et al.*, Nucl. Phys. A **515**, 541 (1990).

[18] X. Ledoux, Ph.D. thesis, University of Caen, 1994.

[19] G.D. Westfall *et al.*, Phys. Rev. C **17**, 1368 (1978).

[20] S. Nagamiya *et al.*, Phys. Rev. C **24**, 971 (1981).

[21] M. Mahi *et al.*, Phys. Rev. Lett. **60**, 1936 (1988).

[22] A.I. Warwick *et al.*, Phys. Rev. C **27**, 1083 (1983).

[23] J.P. Alard *et al.*, Nuovo Cimento A **30**, 320 (1975).

[24] R.E.L. Green, R.G. Korteling, K.P. Jackson, Phys. Rev. C **29**, 1086 (1984).

[25] J. Franz *et al.*, Nucl. Phys. A **510**, 774 (1990).

[26] M.L. Brookes *et al.*, Phys. Rev. C **45**, 2343 (1992).

[27] R. D. McKeown *et al.*, Phys. Rev. C **24**, 211 (1981).

[28] J. Cugnon, J. Vandermeulen, Ann. Phys. Fr. **14**, 49 (1989).

[29] D. Polster *et al.*, Phys. Rev. C **51**, 1167 (1995).

[30] F. Goldenbaum *et al.*, Phys. Rev. Lett. **77**, 1230 (1996).

[31] B. van den Bossche, J. Vandermeulen, Z. Phys. A **348**, 281 (1994).

[32] L. Anderson *et al.*, Phys. Rev. C **28**, 1224 (1983).

[33] K. Kwiatkowski *et al.*, Phys. Rev. C **49**, 1516 (1994).

[34] R.R. Doering *et al.*, Phys. Rev. Lett. **40**, 1433 (1978).

[35] W.G. Lynch, Ann. Rev. Nucl. Part. Sci. **37**, 493 (1987).

[36] M. Lindner, R.N. Osborn, Phys. Rev. **103**, 378 (1956).

[37] R. Wolfgand *et al.*, Phys. Rev. **103**, 394 (1956).

[38] S.B. Kaufmann, S.P. Steinberg, Phys. Rev. C **22**, 167 (1980).

[39] L. Kadi, Ph.D. thesis, unpublished.

[40] J. Fréhaut *et al.*, to be published.

[41] S.B. Kaufmann, E.P. Steinberg, G.W. Butler, Phys. Rev. **20**, 2293 (1979).

[42] G. Rudstam, Z. Naturf. A **21**, 1027 (1966).

[43] R. Silberberg, C.H. Tsao, Astrophys. J. Suppl. **5**, 315 (1973); **25**, 335 (1973).

[44] K. Sümmerer *et al.*, Phys. Rev. C **42**, 2546 (1990).

[45] A.Y. Abul-Magd, W.A. Friedman, J. Hüfner, Phys. Rev. C **34**, 113 (1986).

[46] J. Cugnon, Nucl. Phys. A **389**, 191c (1982).

[47] G.D. Harp *et al.*, Phys. Rev. C **8**, 581 (1973).

[48] D. L'Hôte, J. Cugnon, in *Relativistic heavy ion collisions*, edited by L.P. Csernai, D. Strottmann, Int. Rev. Nucl. Phys., WSPC, 1991.

[49] J. Cugnon, T. Mizutani, J. Vandermeulen, Nucl. Phys. A **352**, 505 (1981).

[50] J. Cugnon, Nucl. Phys. A **462**, 751 (1987).

[51] H.W. Bertini *et al.*, Phys. Rev. **131**, 1801 (1963).

[52] Y. Yariv, Z. Fraenkel, Phys. Rev. C **20**, 2227 (1979).

[53] J. Cugnon, M.-C. Lemaire, Nucl. Phys. A **489**, 781 (1988).

[54] W. Botermans, R. Malfliet, Phys. Rep. C **198**, 115 (1990).

[55] R.G. Stokstad, in *Treatise on heavy ion science*, edited by D.A. Bromley (Plenum Press, New York, 1984), Vol. 3, Chap. 2.

[56] V.F. Weißkopf, D.H. Ewing, Phys. Rev. **57**, 472 (1940); **57**, 935 (1940).

[57] N. Bohr, J.A. Wheeler, Phys. Rev. **56**, 426 (1939).

[58] L.G. Moretto, Nucl. Phys. A **247**, 211 (1975).

[59] L.G. Moretto, Prog. Part. Nucl. Phys. **21**, 401 (1988).

[60] W.J. Swiatecki, Austr. J. Phys. **36**, 641 (1983).

[61] J. Richert, P. Wagner, Z. Phys. A **341**, 171 (1992).

[62] J. Garg, in *Statistical properties of nuclei*, edited by J.R. Huizenga (Plenum Press, New York, 1972).

[63] S. Shlomo, J.B. Natowitz, Phys. Rev. C **44**, 2878 (1991).

[64] O. Bersillon, unpublished.

[65] L. Dresner, Oak Ridge report ORNL-TM-196 (1962).

[66] W.B. Amian *et al.*, Nucl. Sci. Eng. **112**, 78 (1992).

[67] S. Vuillier, Ph.D. thesis, Université de Paris-Sud, Orsay, 1998.

[68] L. Pienkowski *et al.*, *Proc. Winter Meeting on Nuclear Physics*, Bormio, 1993, edited by I. Iori, RSEP Milano.

[69] J. Cugnon, A. Lejeune, P. Grangé, Phys. Rev. C **35**, 861 (1987).

[70] Q.G. Li, R. Machleidt, Phys. Rev. C **49**, 566 (1994).

[71] J. Cugnon, R. Sartor, to be published.

[72] J.-P. Jeukenne, A. Lejeune, C. Mahaux, Phys. Rep. C **25**, 83 (1976).

[73] C. Mahaux, R. Sartor, Adv. Nucl. Phys. **20**, 1 (1991).

[74] L.P. Kadanoff, G. Baym, *Quantum statistical mechanics* (W.A. Benjamin, New York, 1962).

[75] R. Malfliet, Nucl. Phys. A **545**, 3c (1992).

[76] J. Aichelin, Phys. Rep. **202**, 233 (1991).

[77] A. Ono, H. Horiuchi, Phys. Rev. C **51**, 299 (1995).

[78] J.J. Griffin, Phys. Rev. Lett. **17**, 478 (1966).

[79] M. Blann, Ann. Rev. Nucl. Sci. **25**, 123 (1975).

[80] P.E. Hodgson, *Proc. Varenna Conference on Nuclear Reaction Mechanisms*, Editrice Compositori, Bologna, 1982.

[81] M. Mashnik, unpublished.

[82] H. Feshbach, A. Kerman, S.E. Koonin, Ann. Phys. (NY) **125**, 429 (1980).

[83] A.J. Koning, RCN Petten report, to be published.

[84] J. Cugnon, C. Volant, S. Vuillier, Nucl. Phys. A **620**, 475 (1997).

[85] X. Ledoux *et al.*, Phys. Rev. Lett. **82**, 4412 (1999).

[86] W. Wlazlo *et al.*, *Proceedings of the XXXVII International Winter Meeting on Nuclear Physics*, Bormio, 1999, edited by I. Iori, RSEP Milano.